Energy 168 (2019) 43–56

Contents lists available at ScienceDirect

Energy

journal homepage: www.elsevier.com/locate/energy

On increasing the thermal mass of a salinity gradient solar pond with external heat addition: A transient study

Sayantan Ganguly [a, *], Abhijit Date [b], Aliakbar Akbarzadeh [b]

[a] Environmental Hydrogeology Group, Department of Earth Sciences, Utrecht University, Princetonlaan 8A, 3584CB Utrecht, the Netherlands
[b] Energy Conservation and Renewable Energy Group, School of Engineering, RMIT University, PO Box 71, Bundoora, Victoria 3083, Australia

ARTICLE INFO

Article history:
Received 29 June 2018
Received in revised form
20 November 2018
Accepted 21 November 2018
Available online 26 November 2018

Keywords:
Salinity gradient solar ponds
Solar thermal energy
Thermal mass
Evacuated tube solar collectors
Thermal efficiency
Transient modeling

ABSTRACT

In salinity gradient solar ponds (SGSPs) solar thermal energy is mainly stored in the lower-convective zone (LCZ) the volume of which defines the thermal mass of storage. The present study explores the provision of increasing the heat storage in a SGSP by increasing the thermal mass of it. It also addresses the method of enhancing the thermal performance of a SGSP by increasing the thermal mass, while adding heat from external sources. Earlier studies have proved that adding external heat to the SGSP for storage enhances the thermal performance of it significantly. This study aims to prove that increasing the thermal mass of storage further increases the energy efficiency of a SGSP when external heat is added to it. A hybrid system of a SGSP coupled with evacuated tube solar collectors (ETSCs) is used in this study. Several parameters like storage temperature in LCZ, heat addition flux and heat addition efficiency of ETSC, instantaneous efficiency of SGSP, heat extraction from SGSP are studied in this paper for different cases of with and without heat addition and with normal and enhanced thermal mass. It is found that increasing thermal mass can significantly enhance the thermal performance and efficiency of a SGSP.

1. Introduction

A salinity gradient solar pond (SGSP) is a surface water body of shallow depth with a salinity gradient in downward direction. A SGSP built to capture and store solar thermal energy for long term. Solar radiation incident on the pond surface, while passing through different layers of the pond, is absorbed and converted to thermal energy. SGSPs are typically of depth 3 m or less [1]. Solar radiation reaching beyond that depth is ineffective to convert to thermal energy due to its massive attenuation while passing through water. A SGSP traditionally consists of 3 layers. Typically the bottom most layer of the pond which has the maximum salinity is used as the thermal energy storage zone. This zone is known as the lower-convective zone or LCZ. Convection current in this zone keeps the temperature of the layer uniform. Being the main heat storage zone, this layer has the highest temperature among all the layers in a SGSP. The zone above LCZ, known as the non-convective zone (NCZ) is the insulation layer of the pond. In NCZ the downward salinity gradient is used to suppress the convection currents and minimize heat losses from the storage zone. The NCZ also has a temperature gradient where the temperature increases downwards. The zone above NCZ, known as upper-convective zone (UCZ) is the topmost layer of a SGSP with lowest salinity. Although this layer receives highest solar radiation in SGSP among all, high heat losses due to convection keep the temperature of this zone the lowest among all the layers. The temperature of UCZ is often very close to local ambient temperature [1].

The volume of fluid in the storage zone or LCZ defines the thermal mass of the SGSP which literally means the mass of saline water in which solar thermal energy is stored. Hence increasing the thermal mass of a SGSP implies increasing the heat storage capacity of it. But while increasing the heat storage, the quality of the heat has to be kept intact. This means the temperature of the heat storage should not be compromised while increasing the storage, which otherwise will limit the application of the heat stored for practical purposes. Thermal mass of a SGSP can be increased by increasing the volume of the LCZ of a SGSP. One way of increasing the volume is to increase the width of the pond. But this requires larger occupation of land surface, which is often limited by land availability and other local constraints. The other way to increase the thermal mass is to increase the depth of storage zone. Larger thickness of the storage zone, other than saving land requirements, also has the beneficial effect of lesser daily temperature

* Corresponding author.
E-mail address: s.ganguly@uu.nl (S. Ganguly).

https://doi.org/10.1016/j.energy.2018.11.090

fluctuations [2]. But increasing storage zone depth may have a negative impact on the thermal performance of SGSP, since solar radiation as mentioned earlier does not reach significantly beyond 3 m depth in water. With addition of heat from external sources, it may indeed be possible to enhance the storage and the thermal performance.

Researchers in the past proposed many ways to enhance the thermal performance of a SGSP. This includes recovering heat simultaneously from LCZ and NCZ [1], introduction of an extra additional NCZ to the SGSP [3], using a solar reflector to reflect additional solar radiation to the pond [4] and recovering heat from ground below the solar pond [5] etc. Addition of heat from external sources has also been established as a strong mean to enhance the thermal performance of a SGSP. Numerical investigations of Ganguly et al. [6,7] have shown the heat collected by evacuated tube solar collectors (ETSCs) and transferred to the SGSP significantly enhances the thermal performance of it. Thus SGSPs can be used to store not only the solar thermal energy that is incident on it, but also external heat from other sources. Experimental investigations of [8,9] have also proved similarly that the thermal performance and efficiency of a SGSP is boosted significantly when heat collected by solar thermal collectors is transferred and stored in it. The summary of the previous studies reported in the present paper is listed in Table 1.

This study aims to prove that increasing the thermal mass of a SGSP by increasing storage depth with external heat addition is a way to further enhance the thermal performance and energy efficiency of it. The thermal performance of SGSP here is characterized by temperature development in the LCZ of the SGSP, the instantaneous efficiency of the SGSP and the heat extraction from LCZ. To the best of knowledge of the authors, no existing literature has addressed the provision of increasing the thermal mass of a SGSP to enhance the thermal performance of it.

The specific objectives of the paper are to numerically investigate- 1. whether increasing the thermal mass of a SGSP by increasing the storage depth is a way to increase the thermal performance and efficiency of it. 2. how the thermal mass can be increased with external heat addition and how much does it enhance the thermal performance, 3. with increasing depth how the insulation thickness (i.e. the thickness of the NCZ) has to be adjusted to optimize the thermal performance intact. 4. how does heat removal from the SGSP affect the thermal performance while external heat addition and storage thermal mass is increased.

2. External heat addition to SGSP

Here, source of the external heat is the solar heat collected by evacuated tube solar collectors (ETSCs). ETSCs are glass tubes which collect solar radiation. Fluid flow through the tubes is used to transfer the collected solar energy. The solar energy absorber tubes consist of two concentric glass tubes with a vacuumed annular space between them. The outer surface of the inner tube works as a solar absorber surface. The vacuum inside the annular space works as insulation to minimize heat losses by convection and conduction to a great extent. The water in glass ETSCs are the most widely used ETSCs because of its higher thermal efficiency of solar thermal energy collection than the others, simple construction and low manufacturing costs [10]. ETSCs are efficient solar thermal collectors but they cannot store any heat. They need a separate device to store the heat for long term. Commercially available hot water storage devices like insulated non-pressurised tanks can be used to store heat from solar energy capturing devices. But these are subjected to high heat loss through the walls resulting in around 8 °C drop in temperature drop within a couple of days [11,12]. SGSPs on the other hand are less efficient in collecting solar energy than ETSCs, but they can indeed store the heat for long term (weeks and months) without a significant drop in temperature, typically 5–10 °C in a month [7]. Thus the hybrid system of an SGSP coupled with ETSC gives a nice option to store considerable amount of heat and simultaneously enhancing the thermal performance of a SGSP significantly [6,7].

In the basic arrangement of the coupled system of ETSC with SGSP, water from LCZ is extracted by a diffuser and is pumped through ETSC. While passing through ETSC the solar heat is transferred from ETSC to the fluid from LCZ. Extracted water is then pumped back to the LCZ, after collecting solar heat from ETSC.

The total energy added to the LCZ ($q_a$in W/m^2) of the SGSP from ETSC is calculated using Eq. 1

$$q_a = \frac{\eta_{et}}{100} \times R \times H_{et} \tag{1}$$

Table 1
Summary of the previous studies related to the present paper.

Ref. no.	Journal article/Book chapter	Objective
[1]	Date et al. (2013)	Enhancing thermal performance of a SGSP by extracting heat from NCZ and LCZ.
[2]	Lu et al. (2001)	Experimental investigation of a thermal desalination system coupled with a SGSP in El Paso as a heat source.
[3]	Husain et al. (2012)	Introducing an additional NCZ to a SGSP and enhancing the thermal performance.
[4]	Aboul-Enein et al. (2004)	Theoretical and experimental investigation of a SGSP with a mirror to reflect additional solar radiation to enhance the thermal performance.
[5]	Ganguly et al. (2017)	Recovering the heat lost to the ground below solar pond
[6]	Ganguly et al. (2017)	Exploring the provision to add external heat to the SGSP
[7]	Ganguly et al. (2018)	Numerical investigation of a SGSP coupled with ETSCs to enhance thermal performance
[8]	Bozkurt and Karakilcik (2012)	Experimental investigation of daily performance of a SGSP coupled with flat plate solar collectors.
[9]	Alcaraz et al. (2018)	Experimental investigation of heat extraction and heat supply processes for a SGSP coupled with solar thermal collectors.
[10]	Bidhihardjo and Morrison (2009)	Investigation of thermal performance of water-in-glass evacuated tube solar collectors for solar water heaters
[11]	Cruickshank and Harrison (2010)	Experimental analysis of heat loss characteristics for a solar domestic hot water storage system.
[12]	Hasnain (1998)	Review of sustainable thermal energy storage technologies for space and water heating applications
[13]	Bidhihardjo et al. (2003)	Experimental and numerical study of thermal performance of a solar water heater by collector efficiency, the tank heat loss coefficient and the natural circulation flow rate through the ETSC.
[14]	Bryant and Colbeck (1977)	Investigation of thermal performance of a SGSP in London
[15]	Ganguly et al. (2018)	Numerical investigation of effectiveness of the insulation used for a SGSP.
[16]	Date and Akbarzadeh (2013)	Book chapter on the fundamentals of the theory of solar pond and their applications
[17]	Wang and Akbarzadeh (1982)	Numerical study on the thermal performance of a SGSP and effect of different parameters.
[18]	Amigo et al.(2017)	Numerical and experimental study on the transient temperature distribution of a SGSP and ground below it.
[19]	Amigo et al.(2018)	Numerical modeling of Ground heat storage below a SGSP under constant heat demand
[20]	Khalilian et al.(2018)	Numerical investigation of transient thermal performance of a SGSP under different heat extraction modes

Where R is the ratio of the aperture area of ETSC to the SGSP floor area, η_{et} is the efficiency of the ETSC (in %), and H_{et} is the incident solar radiation on the ETSC (in W/m^2). According to [10] for a SGSP coupled with ETSC, η_{et} can be defined as a function of incident solar radiation and the difference between LCZ temperature and ambient temperature, given by

$$\eta_{et} = \left\{0.536 - 0.8240\frac{(T_{lcz} - T_{atm})}{H_{et}} - 0.0069\frac{(T_{lcz} - T_{atm})^2}{H_{et}}\right\} \times 100 \tag{2}$$

Where T_{atm} is the ambient temperature (in °C) and $T_{lcz}$is the instantaneous LCZ temperature (in °C). The heat added to the SGSP is also proportional to the ratio (R)

$$R = \frac{A_{et}}{A_{sp}} \tag{3}$$

Here A_{sp} and A_{et} are the surface area of the solar pond (in m^2) and the aperture area of the ETSCs (in m^2), respectively. Note here that equation (2) is an empirical equation derived from the experiments of Budihardjo et al. [13] on a solar collector consisting of 21 ETSCs of absorber diameter 37 mm and spaced 70 mm apart. The experiments consisted of energy gain measurements across solar noon when solar radiation level and solar incidence angle are approximately constant. The measurements were taken for temperature difference to incident solar radiation ratio ($\frac{T_{lcz}-T_{atm}}{H_{et}}$ here) ranging between 0.01 and 0.05. The coefficients were determined from separate measurements of the tube heat loss coefficients.

3. Mathematical and numerical modeling for transient thermal performance of the SGSP

The mathematical model for energy balance in the SGSP coupled with ETSC is described by the following one-dimensional (1D) transient partial differential equation (PDE)

$$\frac{\partial E_X}{\partial t} = \frac{\partial q_X}{\partial X} + H_X + Q_{eX} - Q_{aX} \tag{4}$$

Here X represents the distance in the vertical direction (in m),E_X represents the total energy content per unit volume of the SGSP at a depth of $X$from the SGSP surface (in J/m^3), $H_X$is the solar radiation that is absorbed at a depth of $X$from the SGSP surface (in W/m^3), $q_X$is the conductive heat flux (in W/m^2), Q_{eX}represents the heat extracted (in W/m^3) and Q_{aX} represents the heat added (in W/m^3). Note that each term of equation (4) signifies the change of energy content per unit volume at a depth $X$from the SGSP surface.

Equation (4) is solved numerically by finite-difference method to model the thermal performance of the SGSP coupled with the ETSC. Equation (4) can be discretised, rearranged and written as the finite difference equation for energy balance for the nth (sub-) layer of the pond per unit area as

$$\Delta E_n^{\tau+\Delta\tau} = h_n^\tau \times \Delta\tau + q_{n-1}^\tau \times \Delta\tau + q_{n+1}^\tau \times \Delta\tau - q_{en}^\tau \times \Delta\tau + q_a^\tau \times \Delta\tau \tag{5}$$

Where τ is the instantaneous time (in sec); $\Delta\tau$ is the time difference (in sec); $\Delta E_n^{\tau+\Delta\tau}$ (in J/m^2), represents the change in the energy content of nth layer (i.e. layer under investigation) in solar pond after time difference$\Delta\tau$;h_n^τ (in W/m^2) represents the solar radiation energy absorbed by nth layer in solar pond at time τ; q_{n-1}^τ(in W/m^2), represents the conductive heat transfer to or from the division above the nth layer in solar pond at time τ; q_{n+1}^τ (in W/m^2) represents the conductive heat transfer to or from the division below the nth layer in solar pond at time $\tau$and q_{en}^τ(in W/m^2) represents the heat extracted from the LCZ at time τ.

The change of energy content of the nth layer on the left hand side (LHS) of equation (5) is modelled by the following equation

$$\Delta E_n^{\tau+\Delta\tau} = \rho_n \times \Delta X_n \times c_{pn} \times \left(T_n^{\tau+\Delta\tau} - T_n^\tau\right) \tag{6}$$

Here T_n^τ is the temperature of the nth layer of the SGSP at an instant τ (in K), $T_n^{\tau+\Delta\tau}$is the temperature of the nth layer of the SGSP after time difference $\Delta\tau$(in K), c_{pn} is the specific heat capacity of the nth layer (in J/kg·K), $\Delta X_n$is the thickness of the nth layer (in m), ρ_n is the density of the nth layer (in kg/m^3).

The solar radiation absorbed at each layer in the solar pond (h_n^τ), in the first term on the right hand side (RHS) of equation (5) is estimated by the following equation

$$h_n^\tau = H_{n-1}^\tau - H_{n+1}^\tau \tag{7}$$

Where H_{n-1}^τ and $H_{n+1}^\tau$are the solar radiation flux that reaches the (n-1)th and (n+1)th layers of the SGSP at time τ, respectively (in W/m^2). The solar radiation flux is estimated by the equation given by Ref. [14]

$$H_n^\tau = \left(H_{hs}^\tau - H_{hs}^\tau \times L_r\right) \times (0.36 - 0.08\ln[X_n]) \tag{8}$$

Here $H_{hs}^\tau$is the global solar radiation flux incident on a horizontal surface at timeτ (in W/m^2), X_n is the path length of light in solar pond to the end of the nth sublayer (m) and $L_r$is the reflective loss fraction from SGSP surface to the atmosphere.

The heat conduction flux terms or the second and third terms on the RHS in equation (4) are modelled by following Fourier's law of heat conduction and are given by

$$q_{n-1} = \frac{T_n^\tau - T_{n-1}^\tau}{\frac{\Delta X_n}{2k_n} + \frac{\Delta X_{n-1}}{2k_{n-1}}} \tag{9}$$

$$q_{n+1} = \frac{T_n^\tau - T_{n+1}^\tau}{\frac{\Delta X_n}{2k_n} + \frac{\Delta X_{n+1}}{2k_{n+1}}} \tag{10}$$

Here T_{n-1}, T_n, T_{n+1} is the temperatures of the (n-1)th, nth and (n+1)th layer of the SGSP, respectively (in K); k_{n-1}, k_n, $k_{n+1}$is the thermal conductivities of the (n-1)th, nth and (n+1)th layer of the SGSP, respectively (in W/m·K); ΔX_{n+1}, ΔX_{n+1} and $\Delta X_{n+1}$are the thicknesses of the (n-1)th, nth and (n+1)th layer of the SGSP, respectively (in m).

The heat extraction in the fourth term on the RHS of equation (5) is modelled by following equation

$$q_{en}^\tau = j_{mf} \times c_{pf} \times \left(T_n^\tau - T_{f\ \ n-1}^\tau\right) \tag{11}$$

Here j_{mf} is the mass flux of the heat extraction fluid (HEF) (in kg/m^2/s), $c_{pf}$is the heat capacity of the HEF (J/kg·K). The HEF here flows from (n-1)th to nth layer and collects the heat of the layer getting heated up to its temperature.

The fifth term on the RHS of equation (5) or the heat addition from the external sources (ETSCs here) is modelled by equation (1) as stated before. The whole solution procedure is presented is Fig. 1 as a flow chart.

The hybrid system of SGSP coupled with ETSC in the present study is located at Melbourne, Australia and is schematically shown in Fig. 2. In the basic arrangement the depth of the SGSP is 3 m in

which the thicknesses of the UCZ, NCZ and LCZ are equal to 0.3 m, 1.2 m and 1.5 m, respectively. The surface or bottom area of the SGSP is 50 m^2. The surface area of the Melbourne SGSP is large enough as compared to the sides. Hence the heat loss from the side walls of the pond can be neglected as compared to the heat loss from the bottom of the pond [1,5,6]. The SGSP is insulated by a 20 cm layer of polystyrene at the bottom The density, thermal conductivity, and specific heat of polystyrene used for insulation are 35 kg/m^3, 0.03 W/m·K and 1400 J/kg·K [15]. The salinity of water in UCZ is assumed to be 2%, whereas the same in LCZ is considered equal to 20%. In NCZ which is the gradient layer or the insulation layer for the storage zone, salinity is assumed to increase downwards from 2% to 20%. It should be noted here that the salinity of a SGSP evolves with time because of the vertical salinity gradient and there is a constant diffusion of salt in the upward direction. According to Date and Akbarzadeh [16] for a sodium chloride SGSP the rate of upward diffusion flux is around 20 kg/m^2/year. Thus the salinity of the top layers increase and the bottom layers decline over the period of operation of a SGSP which may extend over months or years. In this study it is assumed that the salinity of the SGSP is maintained by replacing the diffused salt from the LCZ and removing the diffused salt received by UCZ.

Solar thermal energy which is stored at the storage zone of LCZ is extracted from the pond using in-pond heat exchangers situated in the SGSP. The HEF is passed through the in-pond heat exchangers to remove heat from the SGSP. So controlling the fluid flux through the heat exchangers is the best way to control the heat extraction form the SGSP. The heat transfer effectiveness of heat exchangers is assumed to be 1. This implies that the HEF is heated up to the temperature of the (sub-) layer of the SGSP while passing through it.

The operation of the coupled system of SGSP with ETSC started on 1st October, which is early spring in southern hemisphere. Heat extraction from the SGSP starts 60 days after that [1]. The weather data needed for modeling the thermal performance of a SGSP such as the monthly average daily temperature and solar radiation on a horizontal surface in Melbourne are approximated here adequately using sinusoidal functions and shown in Fig. 3. The local average daily temperature in October in Melbourne is considered the temperature of the whole pond at the start of operation and is taken as the initial condition for solving the finite-difference equation (5). With this initial condition and knowing the incoming solar radiation, equations (5)–(11) are solved repeatedly for each (sub-layer), to derive the temperatures of each layer is estimated at the end of each time increment ($\Delta\tau$).

The present numerical model is a 1D finite-difference heat conduction model. The numerical model in the work of [1] which reports a study for the thermal performance for a SGSP in Melbourne, Australia, has been extended here for the study of hybrid system of the SGSP coupled with the external heat source of ETSCs. One-dimensional models have been applied by several researchers in the past [1,4,6,17–19] and also the model results have been successfully validated with experimental results [18,19] or other numerical modeling results from other studies [20]. For the

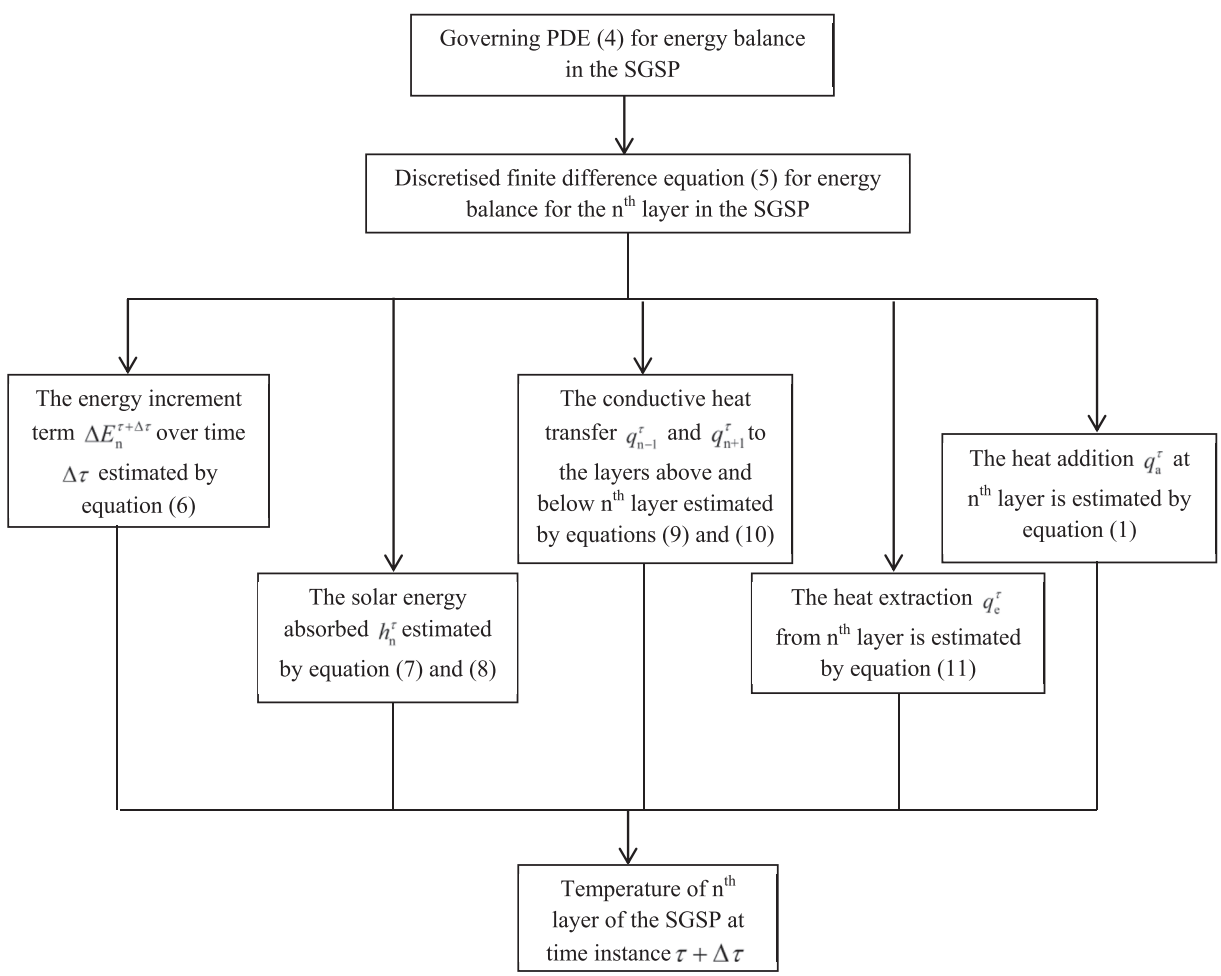

Fig. 1. Flow chart showing the solution procedure for the present study.

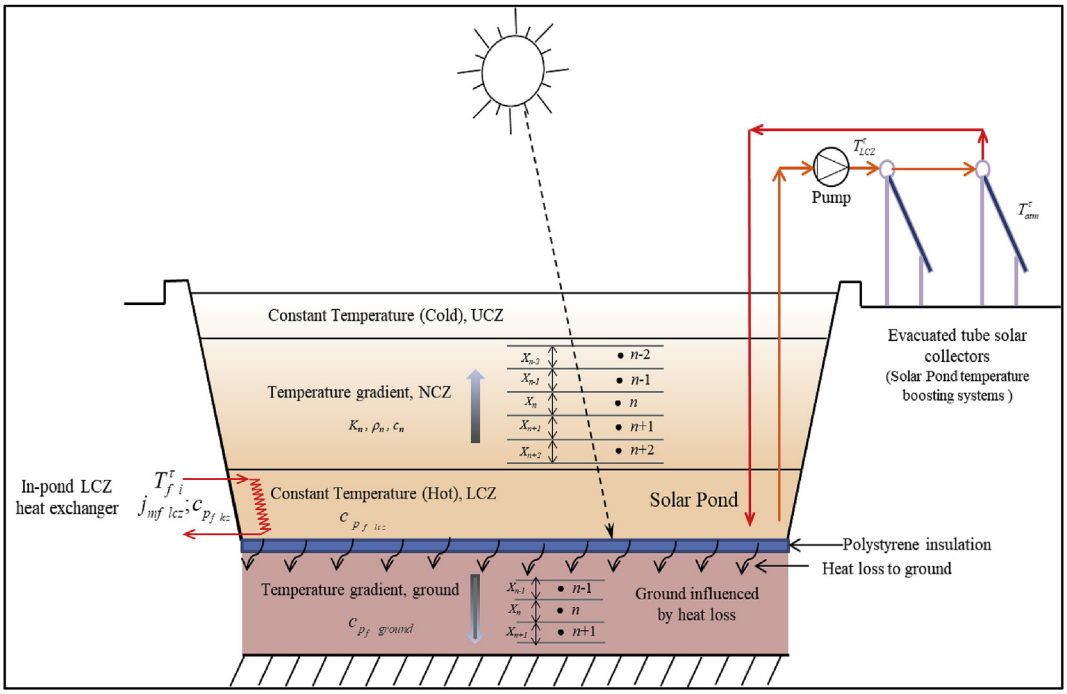

Fig. 2. Schematic diagram of the salinity gradient solar pond with heat addition from evacuated tube solar collectors.

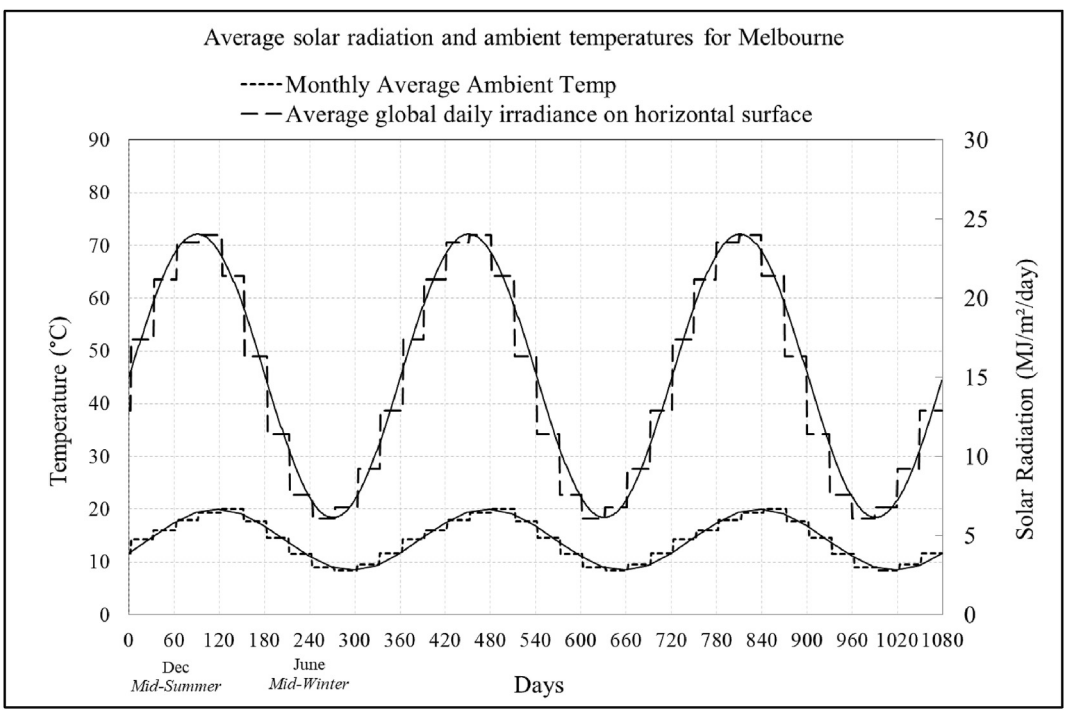

Fig. 3. Monthly average of daily solar radiation on a horizontal surface in Melbourne and monthly average temperature in Melbourne.

Melbourne SGSP and other SGSPs where the side area of the SGSPs are negligible as compared to the bottom/surface area, the geometrical design of the SGSP does not play any significant role as such in the thermal performance of them. So heat loss through the sides can be neglected in modeling their thermal performance. Thus 1D transient model thus can be applied to investigate the thermal performance efficiently. SGSPs where the sides cover significant area as compared to the bottom/surface have significant heat loss from the sides and two-dimensional modeling is necessary in order to model their thermal performance.

For the numerical modeling the UCZ is considered to be a single layer with uniform temperature equal to the monthly average local ambient temperature in the modeling [1,6,7]. Hence the interface of the UCZ and NCZ is considered to be the top boundary of the computational domain with an isothermal boundary condition. The LCZ is also assumed to be a single layer where convective currents

keep the temperature of the layer quite uniform. The gradient layer of NCZ is divided into 8 sublayers of equal thickness of ΔX. Note here that the first node in the NCZ is at a distance $\Delta X/2$ only from the UCZ. Similarly the last node in NCZ is at a distance $\Delta X/2$ from LCZ. So the heat conduction term in equations (9) and (10) for these two layers consists of only one thickness and one thermal conductivity in the denominator.

Wang and Akbarzadeh [17] stated that the heat which is lost from the SGSP to the ground is assumed to be stored ground underneath the SGSP up to a depth of 5 m. The temperature of the ground beyond 5 m below the SGSP can be assumed as the yearly average ambient temperature of that place. Therefore the ground level at a depth of 5 m below the SGSP is considered to be the bottom boundary of the computational domain and this is considered as another isothermal boundary for the numerical model. The 5 m depth of ground is divided into 20 sublayers for the numerical model. As it is mentioned before that heat loss from the sides is neglected, the side boundaries can be treated as adiabatic ones. The transient temperature in the SGSP and ground is estimated at each node located at the centre of the sublayers. The schematic diagram of the computational domain of the SGSP with the numerical grid and heat extraction system is shown in Fig. 4. Readers are referred to the work of [1] for more detailed description of the numerical model.

In the numerical modeling of the SGSP the thermal performance is estimated for a layer of thickness ΔX, after a time increment $\Delta\tau$from the current time instant τ. The time step and thickness of the layer can be of any size, but the stability condition discussed in Ref. [17] has to be satisfied which is given below

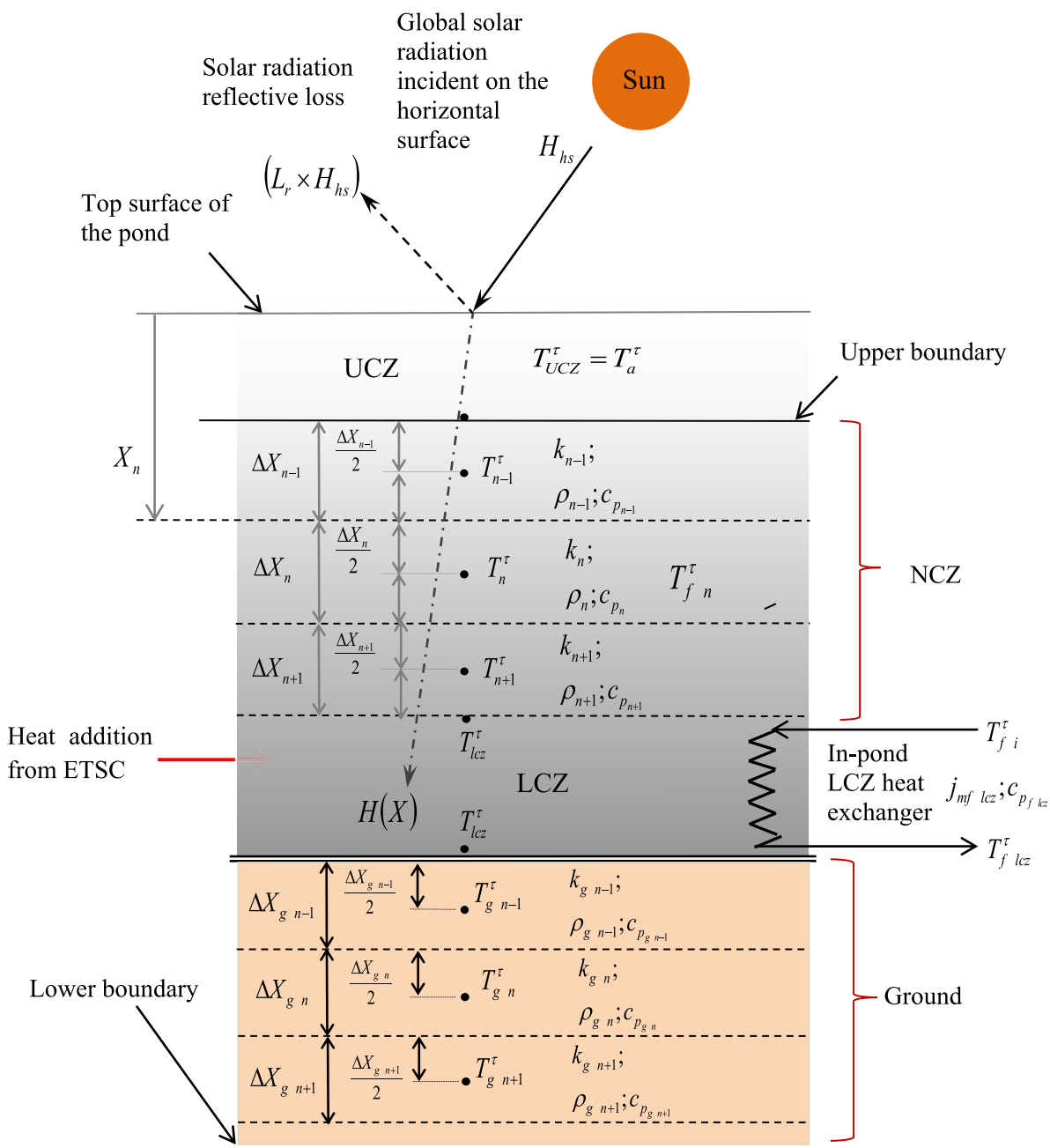

Fig. 4. Schematic diagram showing the different zones of SGSP with the numerical grid and boundaries of the computational domain.

$$\left(\frac{1}{\frac{\Delta X_n}{2k_n}+\frac{\Delta X_{n-1}}{2k_{n-1}}}+\frac{1}{\frac{\Delta X_n}{2k_n}+\frac{\Delta X_{n+1}}{2k_{n+1}}}\right)\times\frac{\Delta\tau}{\rho_n\times\Delta X_n\times c_{p_n}}\leq 1 \tag{12}$$

4. Validation of the present model

In a recent paper [20], which reports the effect of heat extraction mode on the thermal performance of a SGSP located in Urmia city, Iran, the authors have validated the results of transient temperature distribution derived by their 1D numerical model with the results of temperature development reported in Ref. [1]. According to the authors the transient temperature development in the SGSP over a 3 years operation period, derived by both the models agrees with each other very well. As the numerical model from Ref. [1] is extended here for the SGSP with external heat addition, the authors here assume that the numerical model works very well in predicting the thermal performance of a SGSP.

Nevertheless, we compare the results of the present numerical model with an experimental study of a SGSP located in El Paso reported in Ref. [2]. The area and perimeter of the SGSP in El Paso is 3000 m^2 and 250 m, respectively. The total depth of the pond is 3.25 m in which the thickness of the UCZ, NCZ and LCZ are 0.7 m, 1.2 m and 1.35 m, respectively. The local data of annual average monthly ambient temperature and solar radiation in El Paso reported in Ref. [2] given in Table 2 are adequately approximated by sinusoidal functions to predict the temperature development in the SGSP. The present model is applied to predict the temperature development for the El Paso SGSP for a 1 year. Fig. 5 represents the experimental data of temperature development in the LCZ of the SGSP in El Paso reported in Ref. [2] and numerically predicted temperature profile using the present model when no heat is extracted from the SGSP. The transient temperature variation predicted by this model matches quite well with that of the experimental study. The root mean square error (RMSE) of the temperature distribution predicted by this model is about 4.1 °C. In a recent study [18], the authors estimated an RMSE of 4.5 °C for the temperature development derived by their model with that reported in Ref. [2]. The present model thus predicts the temperature development slightly better here. The error of temperature prediction here is attributed to the fact that the effect of groundwater table on the heat transfer is neglected in this model considering it to be deep enough. Also the local meteorological data is approximated here to sinusoidal functions, which gives rise to small errors.

Table 2
Meteorological parameters used for modeling of the El Paso SGSP [2].

SGSP location	Month	Radiation (W/m^2)	Air temperature (C)
El Paso	Jan	145.8	6
	Feb	187.5	8.9
	Mar	245.8	12.8
	Apr	295.8	17.4
	May	325.0	22.1
	Jun	333.3	26.9
	Jul	308.3	27.9
	Aug	283.3	26.7
	Sep	245.8	23.6
	Oct	204.2	17.8
	Nov	158.3	11.3
	Dec	133.3	6.7

5. Temperature development in LCZ with normal and increased storage depth

To fulfill the objectives mentioned in section 1, five cases have been identified which are listed in Table 3. Case 1 represents the base case where the total depth of the SGSP is 3 m where the thicknesses UCZ, NCZ and LCZ are 0.3 m, 1.2 m and 1.5 m, respectively. No heat is added in this case ($R = 0$). Case 2 represents the SGSP where the storage depth of LCZ is increased to 2.0 m. So total depth of the SGSP in this case is increased to 3.5 m. No heat is added in this case either ($R = 0$). In case 3 the depth and thicknesses of all the layers remain same as case 2, but external heat is added from

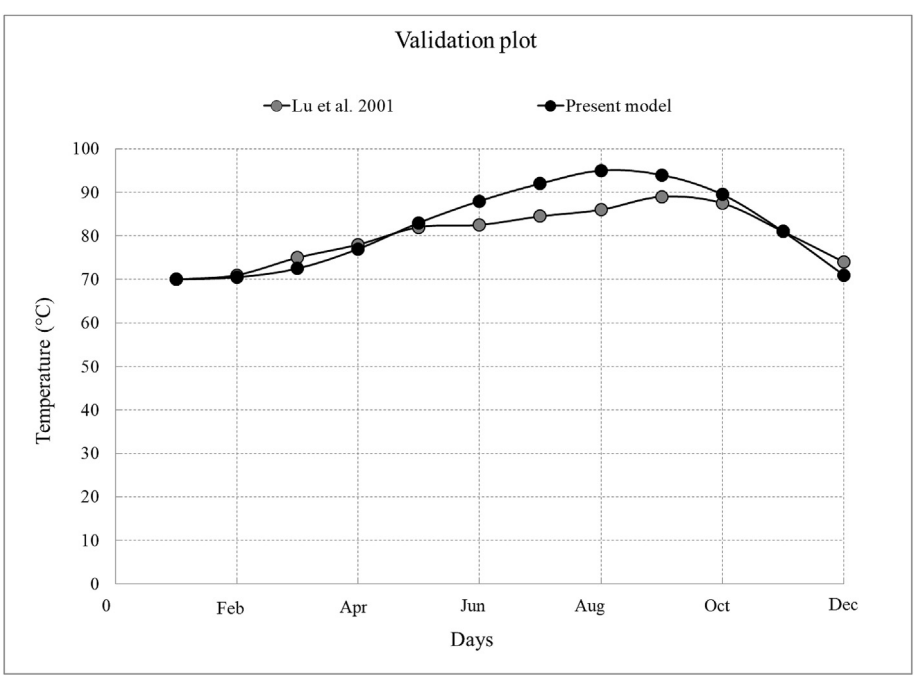

Fig. 5. Comparison of the temperature development in LCZ of the El Paso SGSP reported in Lu et al. (2001) and predicted by the present model.

Table 3
Different cases considered for the modeling.

Cases	UCZ thickness (m)	NCZ thickness (m)	LCZ thickness (m)	Total thickness (m)	R
1.	0.3	1.2	1.5	3.0	0
1A	0.3	1.2	1.5	3.0	0.1
2.	0.3	1.2	2.0	3.5	0
3.	0.3	1.2	2.0	3.5	0.1
4.	0.3	1.2	2.0	3.5	0.5
5.	0.3	1.5	2.0	3.8	0.5

ETSC to the solar pond with a ratio of $R = 0.1$. In case 4 the external heat addition is increased by increasing the ratio R to 0.5 keeping other parameters same as case 3. Finally, in the last case 5, the thickness of the insulation layer (NCZ) is increased to 1.5 m, keeping $R = 0.5$ fixed. Hence, the total depth of SGSP for case 5 becomes 3.8 m. By these 5 cases the variation of thermal performance of the SGSP in Melbourne is investigated. Note that the thermal mass or the surface/bottom area of the Melbourne SGSP is 50 m^2 and the depth of the heat storage zone (LCZ) is 1.5 m for the base case 1 and 2 m for cases 2–5. So the thermal mass or the effective heat storage volume for case 1 is 75 m^3, and for cases 2–5 is 100 m^3. Also, as the LCZ is considered to be a single layer in modeling, having a constant temperature over depth, the depth at which the temperature occurs here depends on the cases. For case 1–2, the temperature at which it occurs at a depth of 1.5–3 m. For cases 3–4 the temperature occurs at a depth of 1.5–3.5 m and for case 5 it occurs at 1.8–3.8 m. The thermophysical properties of the Melbourne SGSP used in the study are given in Table 4 for the UCZ, LCZ and ground below the SGSP. The properties for NCZ depend on the salinity gradient and lie between those of the UCZ and LCZ.

Table 4
Thermophysical parameters of the Melbourne SGSP used in the study.

Parameters	UCZ	LCZ	Ground
Salinity (%)	2	20	–
Thermal conductivity (W/m·K)	0.54	0.59	1.28
Specific heat (J/kg·K)	4094	3492.8	880
Density (kg/m^3)	1020	1200	1460

The vertical temperature profiles of the Melbourne SGSP are presented in Fig. 6 for case 1 and for two fixed times of 6 months and 1 year after the start of the operation. Fig. 6 shows the temperature gradient in the NCZ due to the salinity gradient. Temperature development in the LCZ is shown in Fig. 7 (a) for 3 years of operation for a HEF flux of 0.0002 kg/m^2/s. The ambient temperature in Melbourne and solar radiation data (on the secondary axis) on a horizontal surface in Melbourne is also plotted in the same figure. Note that increasing the ratio R means increasing the aperture area of the ETSC tubes, as the SGSP surface area is fixed. This in turn means increasing means the increasing the number of ETSC tubes. From equation (1) it is evident that as q_a is directly proportional to$R$, as number of ETSC tubes increases, larger amount of heat is added to the SGSP. $R = 0$on the other hand refers to the case of no external heat addition to the pond. According to the work of [6], heat addition from external sources should be performed carefully. Sometimes when due to low heat demand the heat extraction from the SGSP is kept low, during the end of winter the temperature of the fluid adding heat to the pond becomes less that the LCZ temperature. Consequently, instead of adding heat the fluid flux from the ETSC absorbs heat from the SGSP resulting in heat loss and fall of storage temperature. In light of that the HEF flux through the heat exchangers here is kept to a slightly high value of 0.0002–0.00025 kg/m^2/s. Also according to Date et al. [1], there should be a minimum difference of 20 °C between the LCZ temperature and the inlet temperature of the HEF (which equals to the local ambient temperature) for any meaningful use of the heat. Heat extracted from the LCZ below this temperature threshold i.e. lower quality of heat, limits the applications of it for any practical purposes.

Fig. 7 shows that the sinusoidal temperature variation over different seasons of 3 years of operation. Note that the maximum and minimum temperature of storage of the SGSP occurs after mid-summer and mid-winter, respectively i.e. after the maximum and minimum ambient temperature period. This happens due to the thermal inertia of the thermal mass of SGSP.

Evidently the temperature of LCZ fluid increases with increasing R, i.e. increasing amount of heat addition from the ETSC tubes. Also the peak temperature (T_{peak}) and annual average temperature (T_{an}) in the heat storage zone of LCZ of the SGSP depends considerably on

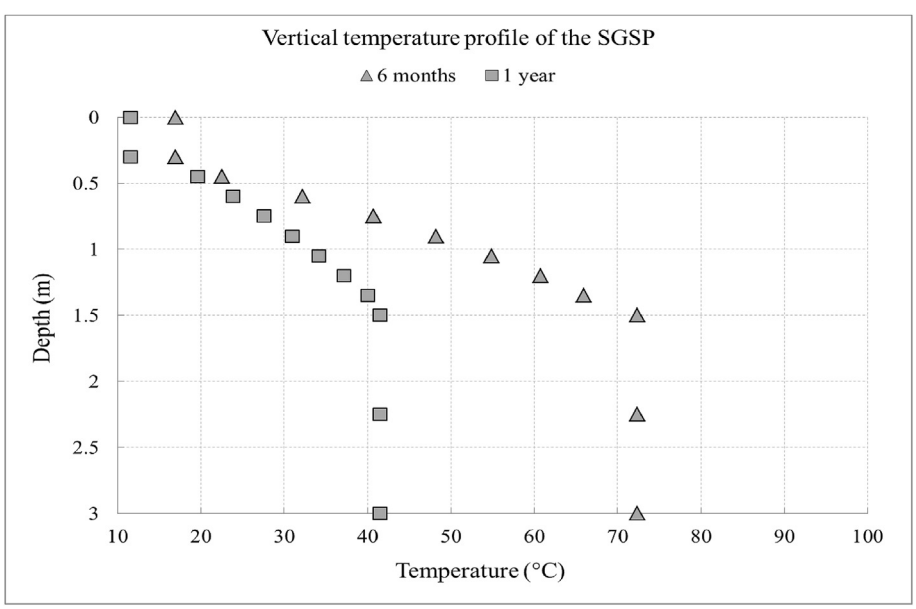

Fig. 6. Vertical temperature profiles of the Melbourne SGSP for case 1, for a heat extraction fluid flux of 0.00020 kg/m^2/s at operation times of 6 months and 1 year.

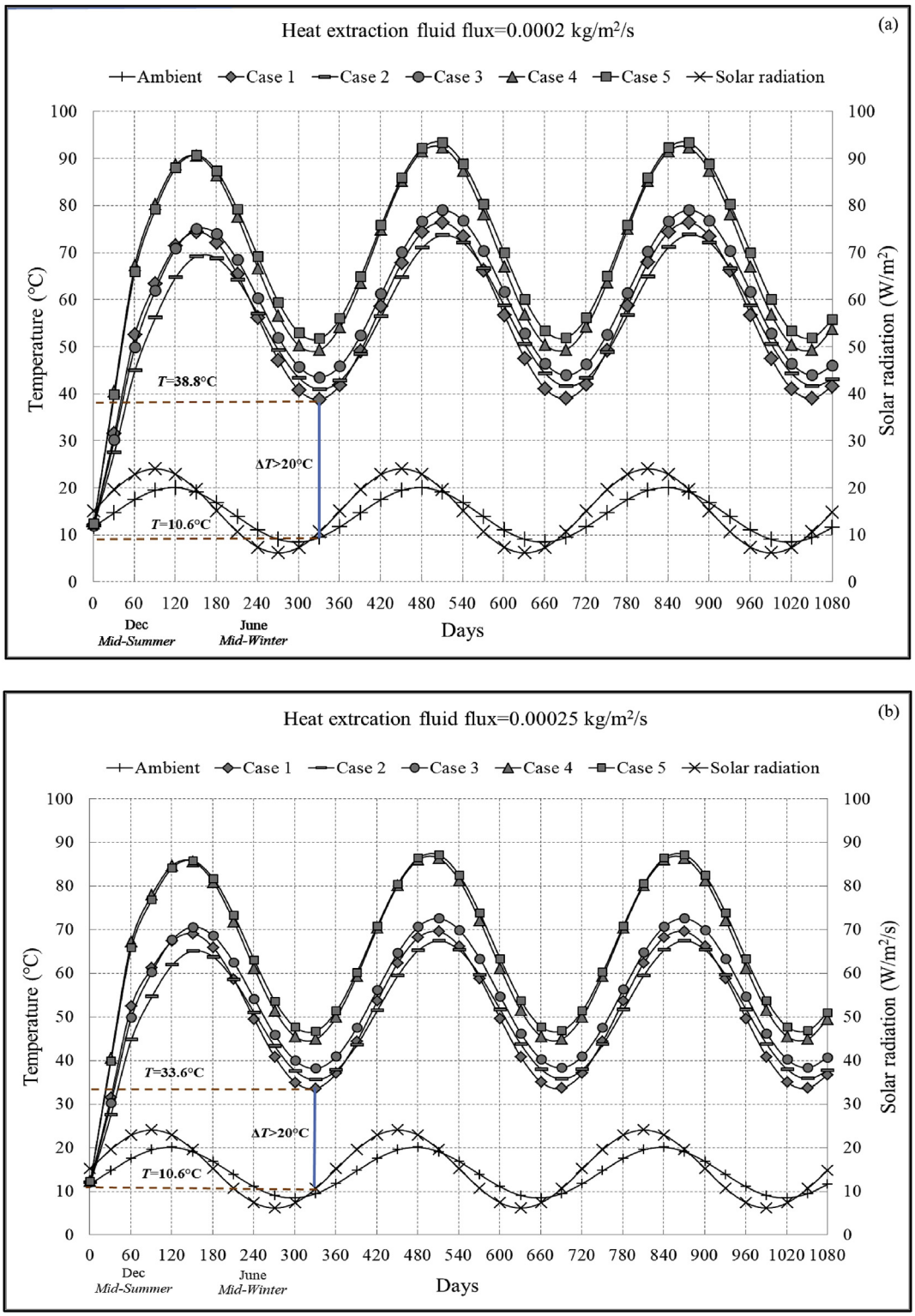

Fig. 7. Temperature development in the LCZ of the SGSP in Melbourne for different cases for heat extraction fluid flux of (a) 0.00020 kg/m^2/s and (b) 0.00025 kg/m^2/s.

the thicknesses of different layers of the SGSP. The T_{peak} and T_{an} in the LCZ, for case1 in the second and third years (first year is ignored since heat removal starts 60 days after start of SGSP operation in the first year) are 76.4 °C and 56.3 °C, respectively. The T_{peak} and T_{an} in the LCZ, for case 2 are 73.7 °C and 54.5 °C, respectively. The reason for fall of temperature in case 2 is the increase of the storage depth or the thermal mass of the SGSP without increase of insulation (NCZ) thickness, which results in larger heat loss from the heat storage zone. So if the thermal mass of the SGSP is increased without sufficient insulation thickness, thermal performance of the pond will be affected. The T_{peak} and T_{an} in the LCZ for case 3 rises to 79 °C and 59.3 °C, respectively, which shows that thermal performance, indicated by the LCZ temperature, has enhanced with external heat addition and is even more than case 1,

in spite of insufficient of insulation thickness. When the external heat addition from ETSC is increased in case 4 ($R = 0.5$) the T_{peak} and T_{an} still increases to 92 °C and 69 °C, respectively. Lastly, in case 5 when the thickness of the insulation zone is increased to 1.5 m, the T_{peak} and the T_{an} reaches 93.3 °C and 70.6 °C, respectively which are the maximum among all the cases. Evidently, with increase in thermal mass of the pond and with increase of external heat addition, thickness of the insulation layer has to be increased in order to extract the best thermal performance from a SGSP. More evidences supporting this suggestion is shown in next sections.

The temperature development on the SGSP for a higher heat removal rate with a HEF flux of 0.00025 kg/m^2/s is shown in Fig. 7(b). The plot also reflects similar trend in result as Fig. 7 (a), except the overall storage temperature of the LCZ is lesser in this case for higher amount of heat removal from it. The minimum temperature of LCZ for all 5 cases here too is maintained well above the limit of 20 °C above the ambient temperature. For HEF flux more than 0.00025 kg/m^2/s (not shown here) it is found that the difference of storage temperature and the ambient temperature at the end of winter falls below 20 °C, which compromises the quality of the heat extracted. This means more heat can be extracted by increasing the HEF flux, but at a lower temperature, limiting the applicability of the extracted heat.

6. Heat addition from ETSC and heat addition efficiency of ETSC

As mentioned earlier, heat addition from the ETSC and the ETSC efficiency are estimated by equations (1) and (2), respectively. To demonstrate the variation of heat addition and ETSC efficiency an additional case 1A is defined here (Table 3). Case 1A is essentially case1 with an external heat addition from ETSC where $R = 0.1$ (since, case 1 did not have any external heat addition). The variation of heat addition from ETSC and ETSC efficiency is presented in Fig. 8 (a)-(d) over 3 years of operation, for cases 1A, 3,4 and 5 (case 2 for external heat addition with $R = 0.1$ is same as case 3).

As the solar radiation varies sinusoidally over different seasons, the ETSC efficiency also varies similarly. It can be seen from all the figures that the ETSC efficiency falls rapidly during the late summer to early winter and starts increasing after mid-winter. The reason behind this is the way the ETSC efficiency is defined in equation (2). The storage temperature in LCZ (T_{lcz}) has a negative impact on the ETSC efficiency, which means that the ETSC efficiency declines when LCZ temperature rises. ETSC efficiency on the other hand rises with rising solar radiation. Hence during this time from late summer to mid-winter, although T_{lcz} decreases, the fall of solar radiation (H_{et}) is much more rapid than that which results in fast decrease in ETSC efficiency. The ETSC efficiency reaches its maximum in mid-summer and minimum in mid-winter. This is for obvious reasons of maximum and minimum values of solar radiation during that time of the year.

The average annual heat addition ($q_{a\ an}$) from the ETSC to the SGSP in the second and third year of operation for a HEF flux of 0.0002 kg/m^2/s equals to 4.6 W/m^2 for case 1A. This amounts to a total heat addition of 145 MJ/m^2 of heat in a year. The $q_{a\ an}$ increases to 4.9 W/m^2 for case 3 amounting to a total heat addition of 154.5 MJ/m^2 in a year. This implies an increase of 6.6% of heat addition annually. Hence, when heat addition from ETSC kept

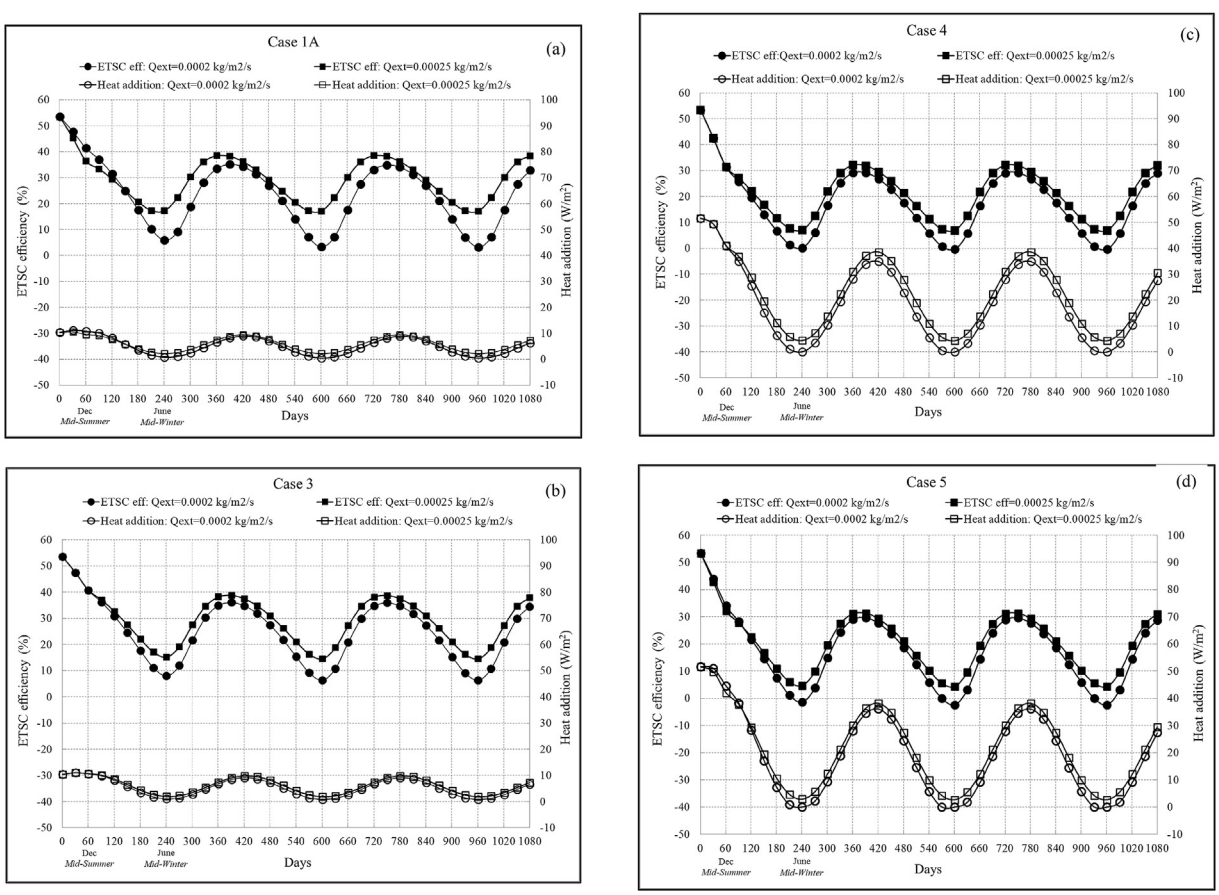

Fig. 8. The thermal efficiency of the ETSC and the heat addition from the ETSC to LCZ for different cases and for HEF flux of 0.00020 kg/m^2/s and 0.00025 kg/m^2/s.

constant ($R = 0.1$, here) and thermal mass is increased, the ETSCs add slightly more heat. This happens due to slight increase of ETSC efficiency estimated by equation (2), which in turn occurs due to reduction of storage temperature in LCZ. The $q_{a\ an}$ is increased to 17 W/m^2 (equals to 536.1 MJ/m^2, a year) in case 4 for obvious reasons of heat addition with 5 times more ETSCs ($R = 0.5$) than case 3. The $q_{a\ an}$for case 5 reduces a little to 16.5 W/m^2, which equals to a total heat addition of 520.3 MJ/m^2 a year. This happens due to slight increase in temperature in LCZ resulting from increase of insulation thickness in case 5.

The $q_{a\ an}$ for case 1A for a HEF flux of 0.00025 kg/m^2 s rises to 5.7 W/m^2 which amounts to a total heat addition of about 180 MJ/m^2 per year. The increase of heat addition in this case is attributed to reduction of LCZ temperatures due to larger heat extraction from SGSP in this case. The $q_{a\ an}$for cases 3, 4 and 5 for this heat removal rate becomes 5.8 W/m^2, 21 W/m^{2}and 20 W/m^2, respectively. The heat addition from ETSC here follows a similar trend for different cases as the previous one, because of similar reasons.

The annual average efficiency ($\eta_{a\ an}$) of the ETSC in case 1A in the second and third year of operation with a HEF flux of 0.0002 kg/m^2/s, equals to 21.5%. This means 21.5% of the solar thermal energy that is incident on the ETSC coupled with the SGSP can be supplied to the LCZ of the SGSP. The $\eta_{a\ an}$in case 3 rises to 23% owing to the decrease of LCZ temperature as mentioned above. Interestingly when the external heat addition is increased by increasing R to 0.5 in case 4, there is a drastic downfall of the ETSC efficiency due to increase of LCZ temperature. The $\eta_{a\ an}$for case 4 and case 5 equals to 15.8% and 15.4%, respectively. The rise of LCZ temperature due to high amount of external heat addition is the reason behind this. The slight difference of $\eta_{a\ an}$ between case 4 and 5 results from the increase of insulation layer thickness in case 5. Hence, the external heat addition to the SGSP should be performed carefully, analysing and optimizing the thermal performance and efficiency of the SGSP while adding heat. Increasing the heat addition by increasing number of ETSC significantly, leads to considerable reduction in ETSC performance which in turn limits the heat addition and will not be economically profitable.

The $\eta_{a\ an}$for case 1A for a HEF flux of 0.00025 kg/m^2/s increases to 28.5%. The enhancement of the ETSC efficiency again pertains to the way it is defined in equation (2). The reduction in LCZ temperature due to larger heat removal from the storage zone causes larger heat addition efficiency of the ETSC. The $\eta_{a\ an}$ for case 3, 4 and 5 in this case are 28%, 20.4% and 19.2%, respectively.

Note that for HEF flux of 0.0002 kg/m^2/s in case 5, the heat addition flux and heat addition efficiency of ETSC attains a slightly negative value during mid-winter. This happens due to the fact that there is continuous flow of HEF from LCZ to the ETSC regardless of the ETSC and LCZ temperatures. During mid-winter due to drastic decrease of solar insolation, the temperature of HEF from ETSC falls below the instantaneous LCZ temperature. Hence, instead of adding heat the HEF flow results in loss of heat from LCZ which is harmful for the thermal performance of the SGSP and should be avoided. Similar phenomenon was noticed by Ganguly et al. [6] in their study. Also note that when the heat removal in increased by increasing HEF flux 0.00025 kg/m^2/s, this problem of negative heat addition is completely avoided in case 5. Hence, the HEF flux is one of the most important parameters to be decided for the optimal performance of a SGSP.

7. Heat extraction and instantaneous efficiency of a solar pond with normal and increased storage depth

The instantaneous efficiency here is defined as the ratio of the sum of instantaneous changes of energy in the LCZ, NCZ and the ground thickness of 5 m underneath the SGSP, to the amount of solar radiation penetrating the SGSP surface [1]

$$\eta_{\text{inst sp}} = \frac{\Delta E^{\tau}_{\text{lcz}} + \Delta E^{\tau}_{\text{ncz}} + \Delta E^{\tau}_{\text{g}}}{\left(H^{\tau}_{\text{hs}} - H^{\tau}_{\text{hs}} \times L_{\text{r}}\right) \times \Delta\tau} \tag{13}$$

where η_{instsp} is the instantaneous efficiency of the SGSP; $\Delta E^{\tau}_{\text{lcz}}$, $\Delta E^{\tau}_{\text{ncz}}$ and $\Delta E^{\tau}_{\text{g}}$ are the changes in the energy content of LCZ, NCZ and ground beneath the SGSP, respectively (in J/m^2). This equation is valid for approximately a temperature range of 5–95 °C in the SGSP. For a safe operation of the SGSP, the temperatures should not reach the freezing or the boiling conditions at one atmospheric pressure. Hence, this temperature range is suitable for safe and efficient operation of a SGSP.

The instantaneous efficiency of the SGSP for a HEF flux of 0.0002 kg/m^2/s is plotted in Fig. 9 (a)–(e) for cases 1–5. The instantaneous efficiency reaches its maximum value during mid-summer and falls rapidly afterwards till mid-winter, when it reaches its minimum value. Note that the instantaneous efficiency attains a negative value during the winter. Instantaneous efficiency is a measure of the heat absorbed by the SGSP to the heat loss from the SGSP. A negative value of the parameter implies that the heat loss from the SGSP during winter is exceeding the heat absorbed during that time. At the start of winter SGSP contains a large heat reserve from the last summer at a high temperature which triggers larger heat loss. During winter the due to lesser solar radiation, heat absorbed by the SGSP reduces and heat loss from the high temperature reserve increases rapidly. Hence the efficiency of SGSP falls drastically during this time and attains a negative value during mid-winter, if not sufficient amount of heat is removed from the storage zone.

The annual average instantaneous efficiency ($\eta_{sp\ an}$) of the SGSP for case 1 in second and third year is about 15%. This means 15% of the solar radiation which is incident on the SGSP is converted to suppliable thermal energy in the storage zone of SGSP here. The $\eta_{sp\ an}$for case 2 reduces to 14.2% which is again due to larger heat loss due to insufficient insulation thickness. But when external heat is added to the SGSP in case 3 ($R = 0.1$) with larger thermal mass the η_{an}increases to 17.2%. When external heat addition is increased to $R = 0.5$ in case 4, the $\eta_{sp\ an}$enhances to 19.6%. Hence external heat addition here evidently enhances the efficiency of the SGSP. Increasing the insulation layer (NCZ) thickness further to 1.5 m in case 5, increases the η_{an} further to 20.2%. Hence enhancing the thermal mass with external heat addition to the SGSP evidently enhances the thermal efficiency of a SGSP significantly. The increase of the $\eta_{sp\ an}$from case 1 to case 5 is about 35%.

The instantaneous efficiency of the SGSP for a HEF flux of 0.00025 kg/m^2/s is also plotted in Fig. 9 (a)-(e). The instantaneous efficiency for the higher heat removal rate in this case is always slightly higher than the previous one. The $\eta_{sp\ an}$for case 1 here is increased to 17%. The $\eta_{sp\ an}$for case 2, 3, 4 and 5 are 16.7%, 20%, 23.2% and 23.8%, respectively. With the increase of heat removal from the storage zone, the heat reserve of the SGSP is more utilized and large heat losses are avoided caused by to accumulation of heat and increase of storage temperature. Hence, the instantaneous efficiency increases with increasing heat removal. But again HEF flux should be controlled and not to be increased indefinitely to increase the SGSP efficiency, so that the temperature difference between LCZ and ambient is maintained above 20 °C, for applicability of the heat [1]. It can be shown that if the HEF flux is increased to 0.0003 kg/m^2/s, the LCZ temperature for case 1 at the end of winter reaches at a minimum value when the minimum temperature difference criterion is violated. So this high heat removal flux should be avoided

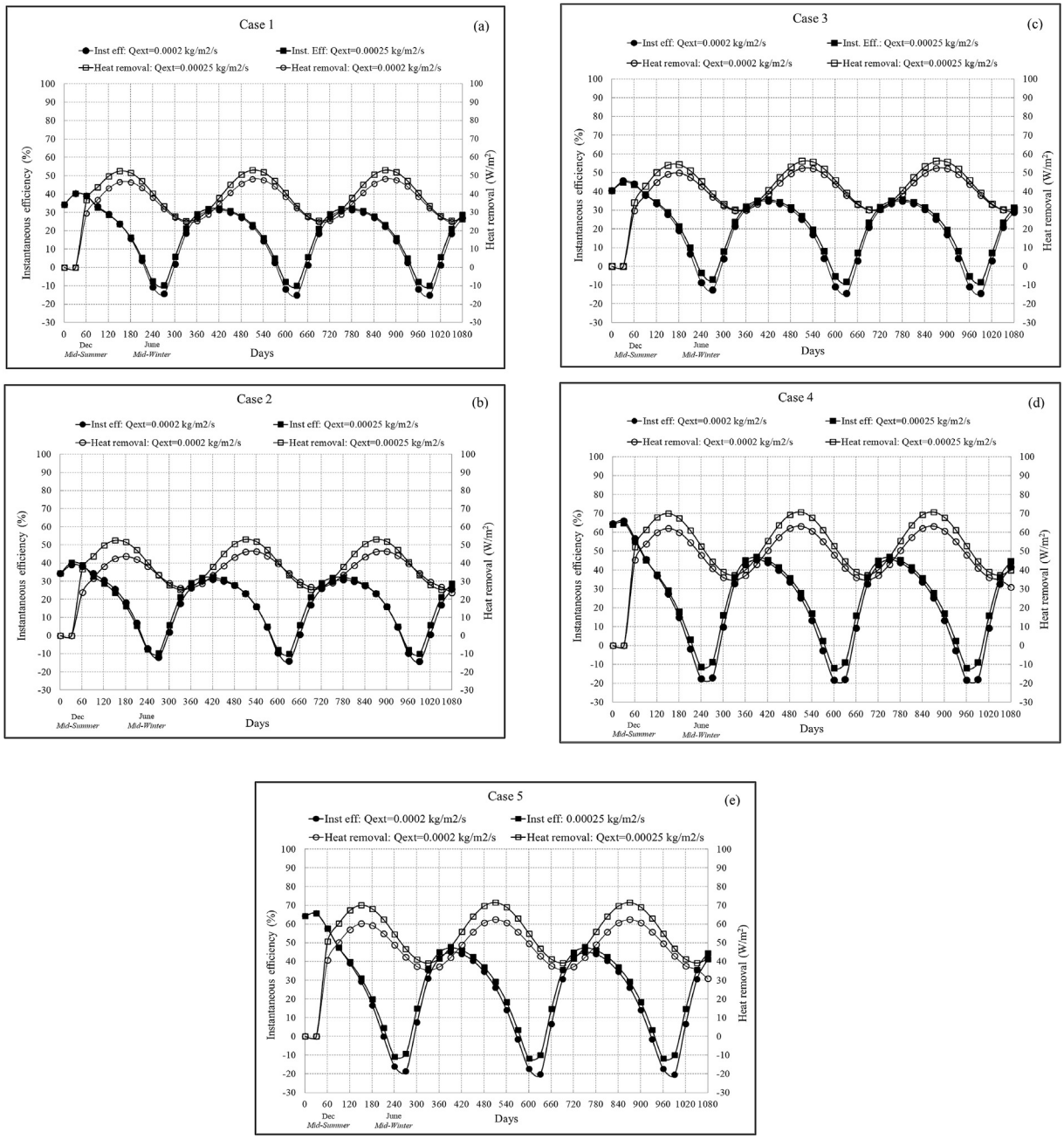

Fig. 9. Heat removal from LCZ and instantaneous efficiency of the SGSP for different cases and for HEF flux of 0.00020 kg/m^2/s and 0.00025 kg/m^2/s.

in that case. The thermal performance should be investigated thoroughly to decide the optimal heat removal rate and HEF flux through the heat exchangers in LCZ. An optimal HEF flux is that one at which the maximum efficiency of the SGSP can be harvested while maintaining the minimum temperature difference criterion.

The annual average heat removal ($q_{e\ an}$) from SGSP in second and third year for case 1, with a HEF flux of 0.0002 kg/m^2/s equals to 36.4 W/m^2 which equals to an annual heat removal of 1147.9 MJ/m^2. The $q_{e\ an}$for case 2 reduces to 36 W/m^2 (annually 1135.3 MJ/m^2) for same reason of $\eta_{sp\ an}$ reduction stated above. With external heat addition ($R = 0.1$) in case 3 the $q_{e\ an}$enhances to 41.5 W/m^2 which equals to annual heat removal of 1308.7 MJ/m^2. This is a heat removal of increase 13% over case 1. With increased heat addition ($R = 0.5$) in case 4 the $q_{e\ an}$also increases to 47 W/m^2 (equals to 1482.2 MJ/m^2 of annual heat removal). Note that while the aperture area of ETSCs is increased 5 times ($R = 0.1$ to 0.5) the $q_{e\ an}$and the $\eta_{sp\ an}$of the SGSP is increased by 5.5 W/m^2 (from 41.5 to 47 W/m^2) and 2.4% (from 17.2% to 19.6%), respectively. With reference to the discussion in section 6 it can be corroborated here that increasing ETSC aperture area significantly does not necessarily enhance the thermal efficiency or heat removal from the SGSP considerably. So increasing the number of ETSCs indefinitely may be economically unbeneficial. Increasing the insulation layer (NCZ) thickness in case 5 to 1.5 m increases the $q_{e\ an}$to 47.3 W/m^2 i. e. 1491.6 MJ/m^2 heat annually. So the gross increase of the heat extraction from the SGSP from case 1 to case 5 is about 30%. The $q_{e\ an}$for a HEF flux of 0.00025 kg/m^2/s, for cases 1–5 becomes 39.2 W/m^2, 39 W/m^2, 43.2 W/m^2, 54 W/m^2 and 55.2 W/m^2, respectively.

It is to be noted here that the construction and material cost of the SGSP will vary with many factors involved in the five cases. The

five cases detailed here involve SGSPs with different depths and thus different volume of fluid in it and different number of ETSC tubes transferring heat to the SGSP. Thus the main factors which will influence the difference of cost for the five cases are (1) cost of the digging, (2) cost of lining, (3) cost of insulation of the bottom and sides of the pond, (4) cost of the salt and (5) cost of the ETSC tubes. For instance the depth of the SGSP in case 2 (3.5 m) and case 5 (3.8 m) is more than the base case (3.0 m) which increases the cost of digging, lining, insulation of sides and salt. Cost of water is also a minor factor which can be added to this. So as a whole the cost of construction of the SGSP increases. Similarly the cost of ETSC tubes in case 3 ($R = 0.1$) and cases 4–5 ($R = 0.5$) increases the overall cost of the hybrid system of the SGSP coupled with the ETSCs. The justification for constructing a SGSP with larger thermal mass (i.e. larger storage depth) and using larger number of ETSCs lies in the fact that the benefit from the SGSP in terms of the thermal performance and efficiency increases significantly in doing so. The economic benefits are much larger than the extra costs involved in the construction.

8. Conclusions

The present paper is aimed to investigate the idea of increasing the thermal mass of a SGSP which is essentially defined by the volume of LCZ in a SGSP. Since increasing surface area has a lot of constraints, increasing the depth of LCZ is suggested here to augment the thermal mass. Enhancing thermal mass has the beneficial effect of larger heat storage capacity of the SGSP and lesser daily temperature fluctuations. But to maintain or to enhance the quality of the heat storage, adding external heat to the SGSP is essential. Increasing thermal mass hereby successfully proved to enhance the thermal performance of a SGSP with addition of external heat. Hence by increasing the thermal mass, both the quantity of heat storage and quality of heat storage can be enhanced. Thermal performance of a SGSP coupled with external heat source of ETSCs in Melbourne here described by the temperature development in LCZ, heat extraction from SGSP and the thermal efficiency of SGSP, has been shown here to improve significantly with heat addition and enhancement of thermal mass. The annual average efficiency and the annual average heat extraction of the Melbourne SGSP for case 5 with enhanced thermal mass and external heat addition increases by 35% and 30%, respectively from the base case 1. The thickness of the insulation layer of NCZ is also proved to be an important parameter while increasing the thermal mass. Without sufficient NCZ thickness, thermal performance of SGSP will be affected and thus it has to be adjusted properly. As traditionally SGSPs are constructed with a depth of around 3 m, it can be considered to be deeper with larger storage volume and storage quality provided external heat is added to it. Proper modeling of the thermal performance is needed while designing a SGSP to ensure harvesting its best efficiency before it is constructed. The numerical modeling study here thus provides a solid basis of enhancing the thermal performance of a SGSP. But we also suggest here that before constructing a SGSP with increased thermal mass practically many parameters have to be optimized to harvest the maximum benefit of it. A detailed cost-benefit analysis is needed to fix different parameters like the dimensions of the pond, the number of ETSCs and the amount of heat to be added etc. Increasing the thermal mass and addition of external heat will definitely increase the cost of the SGSP project as indicated before. But the economic benefits should be estimated in terms of thermal performance, efficiency and the amount and quality of the heat extracted before constructing so that the SGSP project is profitable in the end.

Nomenclature

General signs

A	Area (m^2)
c_{p_n}	Specific heat capacity (J/kg·K)
E	Energy content (J/m^2)
h	Solar radiation flux absorbed by SGSP layers (W/m^2)
H_{et}	Incident solar radiation on ETSC (W/m^2)
k	Thermal conductivity (W/m·K)
L_r	Reflective loss fraction from SGSP surface to the atmosphere
Q_{aX}	Heat added at a depth$X$from SGSP surface (m^2)
Q_{eX}	Heat extracted at a depth$X$from SGSP surface (m^2)
q	Conductive heat flux (W/m^2)
q_a	Total energy added to the LCZ from ETSC (W/m^2)
q_e	Heat flux extracted by heat transfer fluid (W/m^2)
R	Ratio of aperture area of ETSC to the SGSP floor area
T	Temperature (°C)

Greek letters

η	Efficiency
Δ	Difference
τ	Present time (hours)
$\Delta\tau$	Time increment (hours)

Subscripts

a	Addition
e	Extraction
f	Heat extraction fluid
g	Ground
m	Mass flux
n	n^{th} layer/node in solar pond and ground
n-1	layer/node above the nt^h node
n+1	layer/node below the nt^h node
r	Solar radiation
X	Distance from the SGSP surface
an	Annual
a an	Average annual
atm	Atmospheric
aX	Addition at a distance from the SGSP surface
et	Evacuated tubes
eX	Extraction at a distance from the SGSP surface
hs	Horizontal surface
inst	Instantaneous
lcz	Lower-convective zone
ncz	Non-convective zone
sp	Solar pond

Acronyms

ETSC	Evacuated tube solar collectors
HEF	Heat extraction fluid
LCZ	Lower-convective zone
NCZ	Non-convective zone
SGSP	Salinity gradient solar pond
UCZ	Upper-convective zone

References

[1] Date A, Yaakob Y, Date A, Krishnapillai S, Akbarzadeh A. Heat extraction from non-convective and lower convective zones of the solar pond: a transient study. Sol Energy 2013;97:517–28.
[2] Lu H, Walton JC, Swift A. Desalination coupled with salinity-gradient solar ponds. Desalination 2001;136:13–23.
[3] Husain M, Sharma G, Samdarshi SK. Innovative design of non-convective zone of salt gradient solar pond for optimum thermal performance and stability.

Appl Energy 2012;93:357–63.
[4] Aboul-Enein S, El-Sebaii AA, Ramadan MRI, Khallaf AM. Parametric study of a shallow solar-pond under the batch mode of heat extraction. Appl Energy 2004;78(2):159–77.
[5] Ganguly S, Jain R, Date S, Akbarzadeh A. Heat recovery from ground below the solar pond. Sol Energy 2017;155:1254–60.
[6] Ganguly S, Jain R, Date S, Akbarzadeh A. On the addition of heat to solar pond from external sources. Sol Energy 2017;144:111–6.
[7] Ganguly S, Date S, Akbarzadeh A. Investigation of thermal performance of a solar pond with external heat addition. J Sol Energy Eng 2018;140(2):024501 1–6.
[8] Bozkurt I, Karakilcik M. The daily performance of a solar pond integrated with solar collectors. Sol Energy 2012;86:1611–20.
[9] Alcaraz A, Montalà M, Valderrama C, Cortina JL, Akbarzadeh A, Farrana A. Increasing the storage capacity of a solar pond by using solar thermal collectors: heat extraction and heat supply processes using in-pond heat exchangers. Sol Energy 2018;171:112–21.
[10] Budihardjo I, Morrison GL. Performance of water-in-glass evacuated tube solar water heaters. Sol Energy 2009;83(1):49–56.
[11] Cruickshank AC, Harrison SJ. Heat loss characteristics for a typical solar domestic hot water storage. Energy Build 2010;42:1703–10.
[12] Hasnain SM. Review of sustainable thermal energy storage technologies, part I: heat storage material and techniques. Energy Convers Manag 1998;39(11): 1127–38.
[13] Budihardjo, I., Morrison, G.L., Behnia, M., 2003. Development of TRNSYS models for predicting the performance of water-in-glass evacuated tube solar water heaters in Australia. In: Proceedings of ANZSES annual conference, Melbourne, Australia, 2003, electronic proceedings.
[14] Bryant HC, Colbeck I. A solar pond for London? Sol Energy 1977;19(3):321–2.
[15] Ganguly S, Date S, Akbarzadeh A. Effectiveness of bottom insulation of a salinity gradient solar pond. J Sol Energy Eng 2018;140(4):044502 1–5.
[16] Date, S., Akbarzadeh, A., Salinity gradient solar ponds. In: Solar energy sciences and engineering applications, CRC Press; 2013, pp. 195-2018.
[17] Wang YF, Akbarzadeh A. A study on the transient behaviour of solar ponds. Energy 1982;7(12):1005–17.
[18] Amigo J, Meza F, Suarez F. A transient model for temperature prediction in a salt-gradient solar pond and the ground beneath it. Energy 2017;132:257–68.
[19] Amigo J, Suarez F. Ground heat storage beneath salt-gradient solar ponds under constant heat demand. Energy 2018;144:657–68.
[20] Khalilian M, Pourmokhtar H, Roshan A. Effect of heat extraction mode on the overall energy and exergy efficiencies of the solar ponds: a transient study. Energy 2018;154:27–37.